Proc. Natl. Acad. Sci. USA
Vol. 92, pp. 905–909, January 1995
Biochemistry

Vascular endothelial growth factor/vascular permeability factor expression in a mouse model of retinal neovascularization

(angiogenesis/hypoxia/Müller cells/retinopathy of prematurity)

ERIC A. PIERCE*, ROBERT L. AVERY†, ELIOT D. FOLEY*, LLOYD P. AIELLO‡, AND LOIS E. H. SMITH*§

*Department of Ophthalmology, Children's Hospital and Harvard Medical School, Boston, MA 02115; †Neuroscience Research Institute, University of California, Santa Barbara, CA 93103; and ‡Beetham Eye Institute and Research Division, Joslin Diabetes Center and Harvard Medical School, Boston, MA 02215

Communicated by Hector F. DeLuca, University of Wisconsin, Madison, WI, October 7, 1994

ABSTRACT **Neovascular diseases of the retina are a major cause of blindness worldwide. Hypoxia is thought to be a common precursor to neovascularization in many retinal diseases, but the factors involved in the hypoxic neovascular response have not been fully identified. To investigate the role of vascular endothelial growth factor/vascular permeability factor (VEGF/VPF) in retinal neovascularization, the expression of VEGF/VPF mRNA and protein were studied in a mouse model of proliferative retinopathy. RNA (Northern) blot analysis revealed that retinal VEGF/VPF mRNA expression increased 3-fold between 6 and 12 hr of relative retinal hypoxia and remained elevated during the development of neovascularization. *In situ* hybridization localized VEGF/VPF mRNA to cells bodies in the inner nuclear layer of the retina. Immunohistochemical confocal microscopy demonstrated that VEGF/VPF protein levels increase with a time course similar to that of the mRNA. The cells in the inner nuclear layer of the retina that produce VEGF/VPF were identified morphologically as Müller cells. These data suggest that VEGF/VPF expression in the retina plays a central role in the development of retinal ischemia-induced ocular neovascularization.**

Retinal neovascularization is a major cause of blindness in the United States (1). Pathologic retinal angiogenesis is a final common pathway leading to vision loss in diseases such as retinopathy of prematurity (ROP), diabetic retinopathy, and age-related macular degeneration (2–4). Despite the prevalence of these diseases, the biochemical events responsible for retinal neovascularization are not fully understood. It is hoped that a better understanding of the fundamental basis of retinal neovascularization will improve treatment and prevention of retinal vascular diseases.

In these eye diseases, as in tumor growth and wound healing, hypoxia appears to be a common precursor to neovascularization (5, 6). In the 1940s and 1950s, Michaelson (7) and Ashton *et al.* (8) postulated that retinal neovascularization was caused by release of a "vasoformative factor" from the retina in response to hypoxia. Since these initial hypotheses, it has become widely accepted that retinal hypoxia results in the release of factors that influence new blood vessel growth (3). The angiogenic factors responsible for retinal neovascularization, however, have not been conclusively identified.

Vascular endothelial growth factor/vascular permeability factor (VEGF/VPF) is an endothelial cell-specific mitogen that was identified and cloned by several groups of investigators (9–12). The expression of VEGF/VPF is stimulated by hypoxia, and VEGF/VPF has been demonstrated to be required for tumor-associated angiogenesis (13–15). These characteristics make VEGF/VPF an ideal candidate for a retinal vasoformative factor. It has recently been reported that VEGF/VPF levels are elevated in the vitreous of patients with retinal neovascularization (16). It has also been demonstrated that several types of cultured retinal cells secrete VEGF/VPF, and that hypoxia stimulates VEGF/VPF production in some cell types (17–20). VEGF/VPF levels also increase in a primate model of iris neovascularization (21). However, the location and time course of VEGF/VPF expression in association with retinal neovascularization has not been delineated nor has it been determined if VEGF/VPF has a direct role in the induction of retinal neovascularization.

The goal of the present study was to examine the role of VEGF/VPF in retinal neovascularization by studying the time course and location of VEGF/VPF expression in a mouse model of proliferative retinopathy (22). In this model, mice are exposed to hyperoxia, resulting in obliteration of the posterior retinal vessels. The mice are then returned to room air, which is presumed to cause relative hypoxia of the now nonperfused retina, producing a quantifiable neovascular response in 100% of animals. Using this model, the expression of VEGF/VPF mRNA and protein were studied by RNA (Northern) blot analysis, *in situ* hybridization, and immunohistochemical confocal microscopy. These data demonstrate the role of VEGF/VPF in an animal model of retinal neovascularization, which has not previously been done to our knowledge.

EXPERIMENTAL PROCEDURES

Mouse Model. The study adhered to the "Association for Research in Vision and Ophthalmology Statement for the Use of Animals in Ophthalmic and Vision Research." To produce retinal neovascularization, litters of 7-day-old [postnatal day 7 (P7)] C57BL/6J mice with nursing mothers were exposed to 75 ± 2% oxygen for 5 days and then returned to room air at age P12 as described (22). Mice of the same age kept in room air were used as controls. Flat-mounted, fluorescein-conjugated dextran-perfused retinas were examined to assess the retinal vasculature (22).

***In Situ* Hybridization.** For *in situ* hybridization studies, mice at different time points during the induction of neovascularization were deeply anesthetized with Avertin and sacrificed by perfusion through the left ventricle with 4% paraformaldehyde in phosphate-buffered saline. Eyes were enucleated, fixed in 4% paraformaldehyde at 4°C overnight, and embedded in paraffin. Serial 6-μm sections of the whole eyes were placed on microscope slides, and the slides were stored at 4°C. Several slides from each eye were also stained with either hematoxylin alone or periodic acid/Schiff reagent (PAS) and hematoxylin.

Tissue sections were prehybridized and hybridized as described (23). An ^{35}S-labeled RNA probe prepared from rat

The publication costs of this article were defrayed in part by page charge payment. This article must therefore be hereby marked "*advertisement*" in accordance with 18 U.S.C. §1734 solely to indicate this fact.

Abbreviations: PAS, periodic acid/Schiff reagent; RPE, retinal pigment epithelium; VEGF/VPF, vascular endothelial growth factor/vascular permeability factor; P7, etc., postnatal day 7, etc.

§To whom reprint requests should be addressed at: Department of Ophthalmology, Fegan 4, Children's Hospital, 300 Longwood Avenue, Boston, MA 02115.

VEGF/VPF cDNA (24) was used to detect VEGF/VPF in the prepared tissue sections. Single-stranded antisense and sense ^{35}S-labeled RNA probes were prepared by *in vitro* transcription with uridine 5′-[α-(^{35}S)thio]triphosphate (New England Nuclear). Specific hybridization was detected by autoradiography with NTB-2 emulsion (Kodak). Hybridizations with labeled sense RNA probe on adjacent serial sections served as controls for nonspecific binding. Slides were counterstained with hematoxylin and photographed with both light and dark-field microscopy.

Northern Blot Analysis. For Northern blot analyses, retinas from mice at different time points during the induction of retinopathy were isolated and frozen immediately in liquid nitrogen. For each time point, 10 retinas from five mice were pooled, and total retinal RNA was prepared (25). RNA (15 μg) from each time point was then electrophoresed on agarose/formaldehyde gels and transferred by capillary technique to Biotrans nylon membranes (ICN). Hybridization was performed with labeled DNA probes according to established methods (26). DNA probes were prepared from the human VEGF/VPF cDNA (11) by the random hexamer labeling method (27) and [α-^{32}P]dATP (New England Nuclear). Washed membranes were exposed to autoradiography film and analyzed on a PhosphorImager (Molecular Dynamics). Total RNA content was normalized at each time point by probing all blots with 36B4 cDNA (28). ImageQuant software (Molecular Dynamics) was used to quantify the VEGF/VPF and 36B4 signals for each lane on the blots.

Confocal Microscopy. For confocal microscopy, eyes were harvested and fixed in paraformaldehyde as described for *in situ* hybridization studies. Sections were then prepared by using a modification of described techniques (29). Briefly, the posterior segments of paraformaldehyde-fixed eyes were embedded in low-melting-point agarose. Thick serial sections (100 μm) were cut and incubated overnight at 4°C with polyclonal anti-VEGF/VPF antibodies (30). Adjacent sections incubated with normal rabbit serum served as controls. After extensive washing, the sections were incubated with anti-rabbit IgG labeled with the fluorochrome CY3. After additional washing, the sections were mounted in *n*-propyl galate and glycerol and imaged with a Bio-Rad 500 confocal microscope.

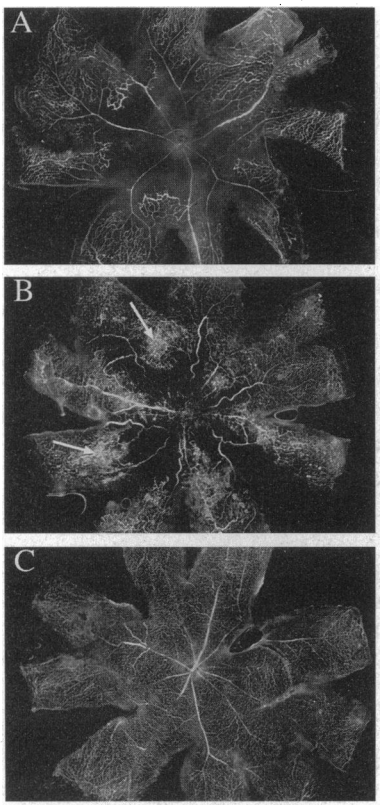

FIG. 1. Flat-mounted, fluorescein-dextran-perfused retinas demonstrating effects of hyperoxia and hypoxia on retinal vasculature (*A*) P12 retina after 5 days of exposure to hyperoxia. (*B*) P17 retina after 5 days of hypoxia. Arrows indicate neovascular tufts extending into the vitreous. (*C*) Normal P17 retina. Note the compete perfusion of retina. (×3.)

RESULTS

Mouse Model of Proliferative Retinopathy. To investigate the role of VEGF/VPF in retinal neovascularization, the expression of VEGF/VPF mRNA and protein in the retina was studied in the mouse model of proliferative retinopathy. In this model, the neovascularization is maximal after 5 days of hypoxia (age P17) and regresses by age P26 (22). Fig. 1 shows representative fluorescein-dextran-perfused retinas from mice during hyperoxia (P12) (Fig. 1*A*) and after 5 days of hypoxia (P17) (Fig. 1*B*); a perfused retina from a normal, age-matched (P17) mouse is provided for comparison (Fig. 1*C*). Note the loss of the central retinal vasculature in Fig. 1*A* and the neovascular tufts in Fig. 1*B*.

Induction of VEGF/VPF mRNA Expression During Neovascularization. The temporal expression of VEGF/VPF mRNA in the retina during hypoxia and the development of neovascular-

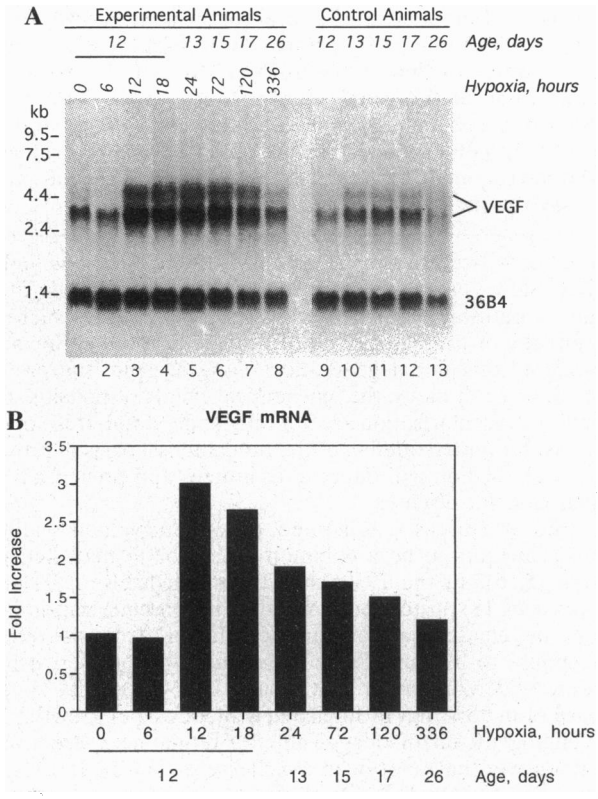

FIG. 2. VEGF/VPF mRNA expression during hypoxia and the development of neovascularization. (*A*) Northern blot analysis. Total retinal RNA (15 μg) from experimental animals after various durations of hypoxia (lanes 1–8) or age-matched normal controls (lanes 9–13) were subjected to Northern blot analysis with VEGF/VPF (VEGF) and control (36B4) cDNA probes. (*B*) Northern blot quantitation. The Northern blot in *A* was analyzed with IMAGEQUANT software. For these calculations, the amount of VEGF/VPF mRNA at each time point was first normalized to its own 36B4 signal. The fold increase over the normalized value for the corresponding age-matched normal control was then calculated. Similar data were obtained from two other Northern analyses (data not shown).

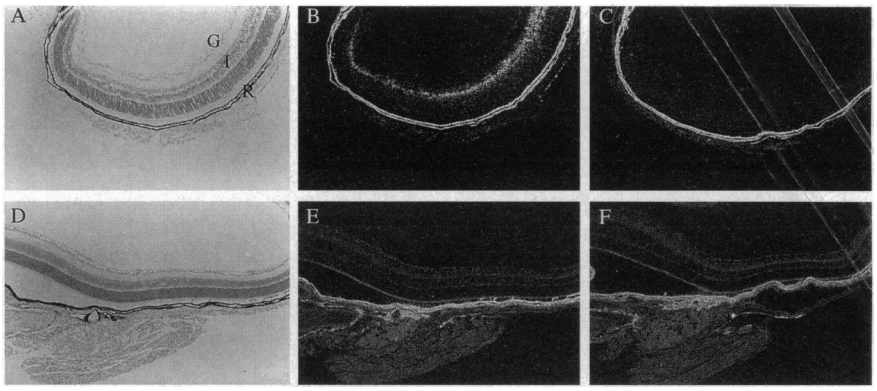

FIG. 3. *In situ* hybridization of VEGF/VPF mRNA expression. Sections from the eyes of animals exposed to 24 hr of hypoxia (*A–C*) and normal age-matched (P13) controls (*D–F*) were analyzed by *in situ* hybridization and photographed with light (*A* and *D*) and dark-field (*B, C, E,* and *F*) illumination. (*A*) Hybridization with antisense probe after 24 hr of hypoxia. The ganglion cell layer (G), inner nuclear layer (I), and the retinal pigment epithelium (RPE) (designated R) are indicated. (*B*) Dark-field image of *A*. (*C*) Control hybridization of adjacent serial section with the sense probe, dark-field image. (*D*) Hybridization with antisense probe, age-matched (P13) normal control. (*E*) Dark-field image of *D*. (*F*) Control hybridization of adjacent serial section with the sense probe, dark-field image. (×12.5.)

ization was evaluated by Northern blot analysis. Fig. 2*A* shows a dramatic increase in VEGF/VPF mRNA levels between 6 and 12 hr after return of experimental P12 mice to room air—that is, after 6 to 12 hr of hypoxia (Fig. 2*A*, lanes 2 and 3). The VEGF/VPF mRNA levels remained elevated for several days and then decreased toward baseline with regression of the retinopathy (P26; Fig. 2*A*, lane 8). Control RNA from age-matched animals raised in room air demonstrated a comparatively constant, low level of VEGF/VPF mRNA (Fig. 2*A*, lanes 9–13). The sizes of the VEGF/VPF transcripts detected in these studies are approximately 3.7 kb and 4.5 kb.

Fig. 2*B* shows the fold increase in VEGF/VPF mRNA for each hypoxic time point compared with age-matched controls after normalization to the 36B4 signal in each lane. PhosphorImager quantitation of the VEGF/VPF mRNA signal on the Northern blot shown in Fig. 2*A* showed a maximal 3-fold increase of VEGF/VPF mRNA at 12 hr of hypoxia compared with normal, age-matched controls.

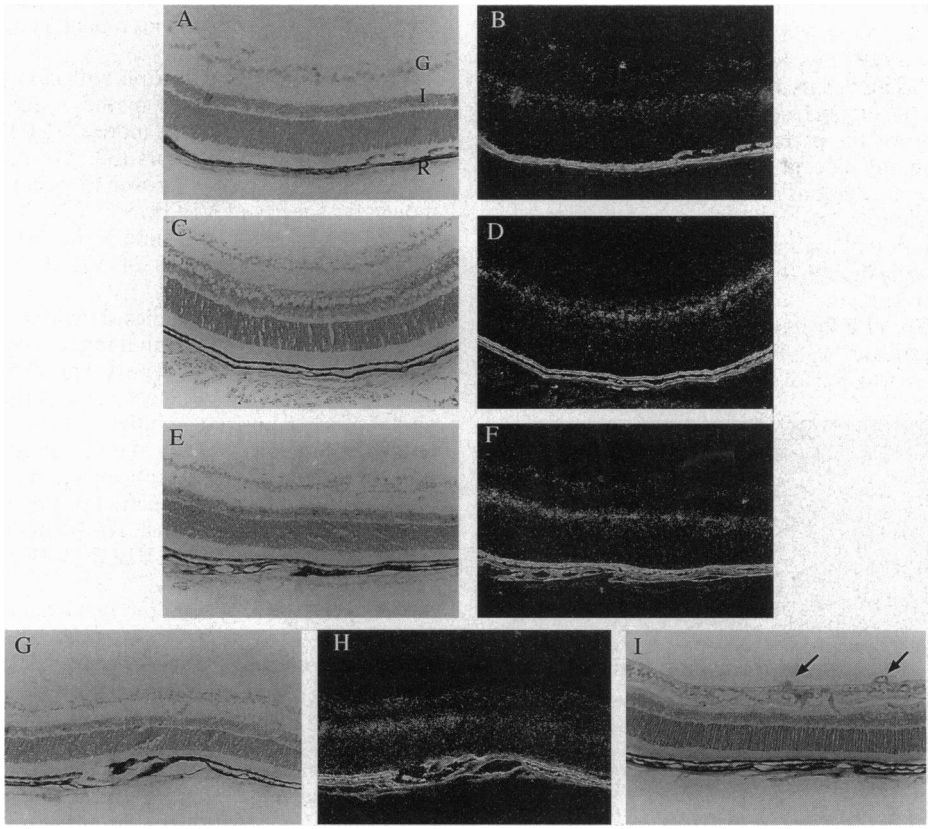

FIG. 4. *In situ* hybridization analysis of VEGF/VPF mRNA expression during the development of neovascularization. Sections from the eyes of animals at the ages indicated were analyzed by *in situ* hybridization and photographed with light (*A, C, E, G,* and *I*) and dark-field (*B, D, F,* and *H*) illumination. All hybridizations shown were performed with antisense probe. The ganglion cell layer (G), inner nuclear layer (I), and RPE (R) are indicated in *A*. (*A* and *B*) Age P12, after 5 days of hyperoxia. (*C* and *D*) Age P13, after 24 hr of hypoxia. (*E* and *F*) Age P15, after 72 hr of hypoxia. (*G* and *H*) Age P17, after 120 hr of hypoxia. (*I*) Serial section adjacent to *G* and *H*, stained with PAS and hematoxylin to demonstrate neovascular tufts (arrows). (×30.)

To determine the location of VEGF/VPF mRNA expression during the development of neovascularization, *in situ* hybridization was performed. Fig. 3 shows the results of a typical *in situ* hybridization performed after 24 hr of hypoxia and in age-matched (P13) normal controls. Hybridization of the hypoxic retinas with antisense probe showed an intense signal for VEGF/VPF mRNA over the inner nuclear layer of the retina and a small amount of labeling over the ganglion cell layer (Fig. 3*A* and *B*). In contrast, age-matched nonhypoxic control retinas showed very little VEGF/VPF mRNA signal (Fig. 3 *D* and *E*). Hybridization with sense probe showed low background in both hypoxic and control retinas (Fig. 3 *C* and *F*, respectively). Note that the RPE has a bright signal on dark-field microscopy due to the presence of pigment granules, and thus probe hybridization over this area cannot be accurately evaluated.

Fig. 4 shows the pattern of VEGF/VPF mRNA expression during the time course of hypoxia and the development of retinal neovascularization. At age P12, just prior to removal of the animals from oxygen, some specific hybridization was seen in the inner nuclear and ganglion cell layers (Fig. 4 *A* and *B*). After 24 hr of relative hypoxia, at age P13, the VEGF/VPF mRNA signal was dramatically increased (Fig. 4 *C* and *D*). After 72 and 120 hr of hypoxia (P15 and P17, respectively), the VEGF/VPF mRNA signal in the inner nuclear layer was still strong, and more mRNA in the ganglion cell layer was detected (Fig. 4 *E–H*). By age P26, little VEGF/VPF mRNA was detected (data not shown). Retinas from age-matched control animals at each time point showed a pattern of hybridization similar to that of the P13 controls shown in Fig. 3 *D–F*. Sense hybridization controls were used in all experiments and demonstrated uniformly low background, as seen in Fig. 3 *C* and *F*.

At time points early in hypoxia, such as after 24 hr of hypoxia (P13), the entire inner nuclear layer showed VEGF/VPF hybridization (Fig. 3 *A* and *B*; Fig. 4 *C* and *D*). The neovascular tufts that develop in this model are concentrated in the middle retina at the junction of the perfused and nonperfused retina (Fig. 1) (22). Fig. 4 shows the pattern of hybridization at P17 (Fig. 4*H*) compared to an adjacent serial section stained with PAS and hematoxylin to demonstrate the neovascular tufts (Fig. 4*I*). The hybridization signal in the inner nuclear layer is concentrated in the non-perfused retina just posterior to the neovascular tufts growing though the inner limiting membrane into the vitreous (arrows).

Stimulation of VEGF/VPF Protein Expression and Cellular Localization. To investigate VEGF/VPF protein expression, immunohistochemistry was performed with confocal microscopy. Fig. 5 demonstrates that VEGF/VPF protein is produced by cells in the inner nuclear layer of the retina, consistent with the results of the *in situ* hybridization studies described above. The additional resolution of confocal microscopy makes it possible to determine that the VEGF/VPF protein is located in cells morphologically consistent with the Müller cells of the retina. This is evident from the staining of cell bodies in the inner nuclear layer, with spindle-shaped processes that span the entire width of the retina (Fig. 5 *A* and *B*) (31). At age P17, after 5 days of hypoxia, more VEGF/VPF is present in experimental (Fig. 5 *A* and *B*) than control (Fig. 5*D*) retinas. The VEGF/VPF staining is specific, as indicated by the low background observed with nonimmune serum (Fig. 5*C*). Further controls with secondary antibody alone revealed no signal above baseline (data not shown). At mouse ages P12 and P27, very little VEGF/VPF protein was detected (data not shown). Staining of the photoreceptor matrices was not observed consistently with different antibody preparations.

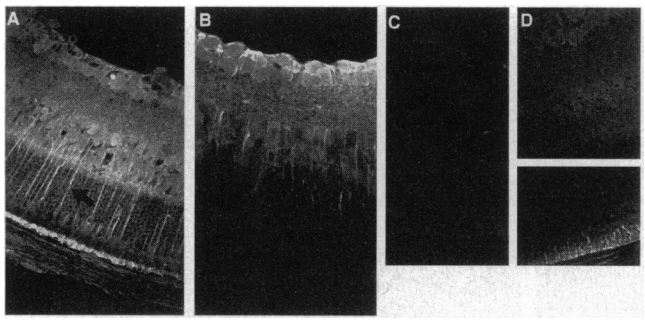

FIG. 5. Confocal immunohistochemistry of VEGF/VPF. Sections from the eyes of animals at the ages indicated were analyzed by immunohistochemistry with anti-VEGF/VPF antibodies (*A*, *B*, and *D*) or nonimmune control (*C*) serum and viewed by confocal microscopy. (*A*) P17, after 120 hr of hypoxia, stained with anti-VEGF/VPF antibodies. Note Müller cell processes spanning retina (arrow). (*B*) Higher power view of *A* showing Müller cell foot plates in inner retina. (*C*) Staining of adjacent serial section with nonimmune serum. (*D*) Normal P17 control, stained with anti-VEGF/VPF antibodies. (*A*, ×21; *B–D*, ×42.)

DISCUSSION

Our data demonstrate that VEGF/VPF is expressed in the retina prior to the development of neovascularization in a mouse model of proliferative retinopathy. The VEGF/VPF mRNA level increases dramatically within 6–12 hr of relative retinal hypoxia and remains elevated until neovascularization develops. The VEGF/VPF mRNA level then declines as the neovascularization regresses to nearly control levels by P26, when the neovascularization has regressed. The levels of VEGF/VPF protein correlate with the mRNA levels. This time course and the localization data discussed below are consistent with a central role for VEGF/VPF in the development of the neovascularization, and thus represents the first reported demonstration of the association between VEGF/VPF expression and retinal neovascularization in an animal model.

Two VEGF/VPF transcripts with sizes of approximately 3.7 and 4.5 kb were detected in these studies. These sizes are consistent with the size of mouse VEGF/VPF messages detected by other investigators (32, 33). Alternative splicing of VEGF/VPF mRNA is known to occur and generates four molecular species of VEGF/VPF (34, 35). Additional studies will be required to determine if the two transcripts detected code for different species of VEGF/VPF and if they are differentially regulated.

In situ hybridization studies show that VEGF/VPF mRNA is produced by cells in the inner nuclear layer of the retina. This is consistent with a prior report that VEGF/VPF mRNA was produced in the inner nuclear layer of the retina in a monkey model of iris neovascularization (21). Of further interest, our data demonstrate that as neovascularization develops, the VEGF/VPF message is concentrated just posterior to the neovascular tufts, at the junction of the perfused and nonperfused portions of the retina. This demonstrates an especially strong correlation between VEGF/VPF expression and retinal neovascularization.

The specific cell type in the inner nuclear layer responsible for VEGF/VPF production has not been previously identified. Our immunohistochemical data demonstrate that VEGF/VPF is produced by cells morphologically consistent with Müller cells. This is evident from the unique morphology of Müller cells, with cell bodies in the inner nuclear layer and radial processes that span the entire retina. The other retinal cells whose cell bodies are present in the inner nuclear layer are all neurons with morphologies distinctly different from the immunostaining pattern observed (31). Müller cells are the principal glial cells of the neural retina. The finding that VEGF/VPF is produced by Müller cells is consistent with their known role as regulators of the extracellular environment of the retina (31). Our data does not eliminate the possibility that other retinal cells also produce VEGF/VPF.

In the mouse model used for these studies, exposure of neonatal mice to hyperoxia causes obliteration of the central retinal vessels. Return to room air is then hypothesized to cause relative retinal hypoxia, which leads to the observed neovascularization (22). This approach to the creation of proliferative retinopathy was first used by Ashton *et al.* (8) and has been used by others more recently (36). While it is hypothesized that the avascular retina is hypoxic in these models, there is no direct evidence that the central, avascular retina is hypoxic following return to room air in the mouse model. There is, however, direct evidence from other animal models of retinal neovascularization that the avascular retina is hypoxic (37, 38). Fluorescein-dextran perfusion of mice exposed to hyperoxia demonstrates complete loss of the retinal capillary bed in the central retina (22). It is a reasonable hypothesis, therefore, that the nonperfused retina is hypoxic in the mouse model.

Given the assumption that the avascular retina is hypoxic in the mouse model, the findings presented here are consistent with those of other investigators, who have shown that VEGF/VPF is regulated by hypoxia. This has been demonstrated in cell culture systems (18), in clinical tumor specimens (13, 14), and in other animal model systems (21). The mechanism by which hypoxia stimulates VEGF/VPF expression has not been determined.

The data presented here provide evidence of a correlation of VEGF/VPF expression with retinal neovascularization suggesting that VEGF/VPF plays a major role in retinal neovascularization. Further studies, however, will be required to determine if VEGF/VPF is directly responsible for retinal neovascularization. Several studies have demonstrated that blocking of VEGF/VPF activity with antibodies can prevent retinal endothelial cell growth *in vitro* and angiogenesis-dependent tumor growth *in vivo* (15, 16). The mouse model of proliferative retinopathy is well-suited to such blocking studies, as it is 100% reproducible (22). If VEGF/VPF is found to be required for retinal neovascularization, then agents that block VEGF/VPF action or expression might be clinically useful to prevent or limit neovascular disease.

In summary, the data presented here demonstrate the association between VEGF/VPF expression and retinal neovascularization in an animal model. In addition, Müller cells have been found to be the predominant producers of VEGF/VPF in the *in vivo* retina. These data, therefore, help clarify the pathogenesis of ischemic retinal vascular disease and elucidate a vasoformative factor hypothesized to exist over 40 years ago (7, 8). An improved understanding of the mechanism by which VEGF/VPF illicits the ischemia-induced neovascular response may eventually lead to improved future therapeutic regimens for these blinding diseases.

We thank Dr. Gabriel Corfas for technical advice about *in situ* hybridization and Richard Sullivan for assistance with tissue preparation and photography. We are grateful to Dr. Napoleon Ferrara for his gift of anti-VEGF/VPF antibodies and human VEGF/VPF cDNA, and to Dr. Brygida Berse and Dr. Donald Senger for their gift of rat VEGF/VPF cDNA. This work was supported in part by grants from the National Eye Institute (K11 EY00343 to E.A.P. and EY08670 to L.E.H.S.), by a grant from the Knights Templar Eye Foundation to E.A.P., and by a grant from the Vitreoretinal Research Institute to R.L.A.

1. Anonymous (1993) *Vision Research, A National Plan: 1994–1998*, A Report of the National Advisory Eye Council (Natl. Inst. Health, Bethesda, MD), DHHS Publ. No. (NIH) 93-3186.
2. Flynn, J. T. (1990) in *Treatment of Retinopathy of Prematurity*, eds. Eichenbaum, J. W., Mamelok, A. E., Mittl, R. N. & Orellana, J. (Year Book Med., Chicago), pp. 81–117.
3. Patz, A. (1982) *Am. J. Ophthalmol.* **94,** 715–743.
4. Bressler, N. M., Bressler, S. B. & Gragoudas, E. S. (1993) in *Principles and Practice of Ophthalmology*, eds. Albert, D. M. & Jakobiec, F. A. (Saunders, Philadelphia), pp. 834–852.
5. Knighton, D. R., Hunt, T. K., Scheuenstuhl, H., Halliday, B. J., Werb, Z. & Banda, M. J. (1983) *Science* **221,** 1283–1285.
6. Folkman, J. & Klagsbrun, M. (1987) *Science* **235,** 442–446.
7. Michaelson, I. C. (1948) *Trans. Ophthalmol. Soc. U.K.* **68,** 137–180.
8. Ashton, N., Ward, B. & Serpell, G. (1954) *Br. J. Ophthalmol.* **38,** 397–432.
9. Senger, D. R., Galli, S. J., Dvorak, A. M., Perruzzi, C. A., Harvey, V. S. & Dvorak, H. F. (1983) *Science* **219,** 983–985.
10. Ferrara, N. & Henzel, W. J. (1989) *Biochem. Biophys. Res. Commun.* **161,** 851–858.
11. Leung, D. W., Cachianes, G., Kuang, W. J., Goeddel, D. V. & Ferrara, N. (1989) *Science* **246,** 1306–1309.
12. Keck, P. J., Hauser, S. D., Krivi, G., Sanzo, K., Warren, T., Feder, J. & Connolly, D. T. (1989) *Science* **246,** 1309–1312.
13. Plate, K. H., Breier, G., Weich, H. A. & Risau, W. (1992) *Nature (London)* **359,** 845–848.
14. Shweiki, D., Itin, A., Soffer, D. & Keshet, E. (1992) *Nature (London)* **359,** 843–845.
15. Kim, K. J., Li, B., Winer, J., Armanini, M., Gillett, N., Phillips, H. S. & Ferrara, N. (1993) *Nature (London)* **362,** 841–844.
16. Aiello, L. P., Avery, R. L., Arrigg, P. G., Keyt, B., Aiello, L. M., Jampel, H. D., Shah, S. T., Pasquale, L. R., Thieme, H., Iwamoto, M. A., Park, J. E., Nguyen, H. V., Ferrara, N. & King, G. L. (1994) *N. Engl. J. Med.* **331,** 1480–1487.
17. Adamis, A. P., Shima, D. T., Yeo, K. T., Yeo, T. K., Brown, L. F., Berse, B. & D'Amore, P. A. F. (1993) *Biochem. Biophys. Res. Commun.* **193,** 631–638.
18. Aiello, L. P., Ferrara, N. & King, G. L. (1993) *Invest. Ophthalmol. Vis. Sci.* **35,** 1868 (abstr.).
19. Simorre-Pinatel, V., Guerrin, M., Chollet, P., Penary, M., Clamens, S., Malecaze, F. & Plouet, J. (1994) *Invest. Ophthalmol. Vis. Sci.* **35,** 3393–3400.
20. Thieme, H., Aiello, L. P., Ferrara, N. & King, G. L. (1994) *Diabetes*, in press.
21. Miller, J. W., Adamis, A. P., Shima, D. T., D'Amore, P. A., Moulton, R. S., O'Reilly, M. S., Folkman, J., Dvorak, H. F., Brown, L. F., Berse, B., Yeo, T. & Yeo, K. (1994) *Am. J. Pathol.* **145,** 574–584.
22. Smith, L. E. H., Wesolowski, E., McLellan, A., Kostyk, S. K., D'Amato, R., Sullivan, R. & D'Amore, P. A. (1994) *Invest. Ophthalmol. Vis. Sci.* **35,** 101–111.
23. Sasson, D. A. & Rosenthal, N. (1993) *Methods Enzymol.* **225,** 384–404.
24. Brown, L. F., Yeo, K. T., Berse, B., Yeo, T. K., Senger, D. R., Dvorak, H. F. & van deWater, L. (1992) *J. Exp. Med.* **176,** 1375–1379.
25. Chomczynski, P. & Sacchi, N. (1987) *Anal. Biochem.* **162,** 156–159.
26. Sambrook, J., Fritsch, E. F. & Maniatis, T. (1989) *Molecular Cloning: A Laboratory Manual* (Cold Spring Harbor Lab. Press, Plainview, NY).
27. Feinberg, A. P. & Vogelstein, B. (1983) *Anal. Biochem.* **132,** 6–13.
28. Laborda, J. (1991) *Nucleic Acids Res.* **19,** 3998.
29. Matsumoto, B. & Hale, I. (1993) *Methods Neurosci.* **15,** 54–71.
30. Houck, K. A., Leung, D. W., Rowland, A. M., Winer, J. & Ferrara, N. (1992) *J. Biol. Chem.* **267,** 26031–26037.
31. Neuman, E. A. (1993) in *Principles and Practice of Ophthalmology*, eds. Albert, D. M. & Jakobiec, F. A. (Saunders, Philadelphia), pp. 398–419.
32. Claffey, K. P., Wilkison, W. O. & Spiegelman, B. M. (1992) *J. Biol. Chem.* **267,** 16317–16322.
33. Breier, G., Albrecht, U., Sterrer, S. & Risau, W. (1992) *Development (Cambridge, U.K.)* **114,** 521–532.
34. Houck, K. A., Ferrara, N., Winer, J., Cachianes, G., Li, B. & Leung, D. W. (1991) *Mol. Endocrinol.* **5,** 1806–1814.
35. Tischer, E., Mitchell, R., Hartman, T., Silva, M., Gospodarowicz, D., Fiddes, J. C. & Abraham, J. A. (1991) *J. Biol. Chem.* **266,** 11947–11954.
36. Penn, J. S., Tolman, B. L. & Lowery, L. A. (1993) *Invest. Ophthalmol. Vis. Sci.* **34,** 576–585.
37. Pournaras, C. J., Tsacopoulos, M., Strommer, K., Gilodi, N. & Leuenberger, P. M. (1990) *Ophthalmology* **97,** 1321–1328.
38. Pournaras, C. J., Tsacopoulos, M., Strommer, K., Gilodi, N. & Leuenberger, P. M. (1990) *Ophthalmology* **97,** 1329–1333.